Optimal Deployment of Multi-Robot Based Regional Positioning System Using Relative Bearing Measurement

Kangwen Lin, Liang Zhang, *Member, IEEE*, Keyue Wu, and Zhaochen Liu

***Abstract*—Recently, the Multi-Robot based Regional Positioning System (MR-RPS) utilizing cooperative localization have emerged as a promising paradigm in Global Navigation Satellite Systems (GNSS)-constraint region: robots first localize themselves using extravagant sensors and then serve as anchors to propagate their noisy positions via cooperative localization and communication with users using accessible devices. However, research on the optimal deployment strategies for bearing-only sensor-based MR-RPS, such as using cameras, remains limited. The bearing-only approach provides a cost-effective and energy-efficient alternative to range-based solutions such as radio systems. This letter proposes a distributed optimal strategy for MR-RPS equipped with bearing-only sensors to provide effective positioning services to the GNSS-limited scenarios. We first employ the Fisher Information Matrix (FIM) and D-optimality as the localziation performance metric using the information received from the Multi-Robot System (MRS). Inspired by the coverage control problem from the Wireless Sensor Network, the optimal deployment of the MRS is then formulated into a locational optimization problem by integrating the value of D-optimality over the entire mission space. A distributed deployment strategy is thus developed, enabling each robot to iteratively compute optimal deployment strategies to enhance the overall performance for stochastically appearing users. Extensive simulations and physical experiments validate the resilience and effectiveness of the proposed method in delivering high-quality positioning services.**

***Index Terms*—MR-RPS, distributed robot systems, optimal deployment, FIM, relative bearing measurement.**

I. Introduction

RECENTLY, the Regional Positioning Systems (RPS) are gaining more and more attention as they can provide a feasible navigation alternative in the GNSS-limited environments, such as the LORAN [1], Locata [2], etc. By leveraging the mobility of the robotic platform (e.g. the mobile vehicles [3], airborne [4] or micro satellite [5]), the MR-RPS can further dynamically extend navigation coverage, eliminate redundant node deployment, and lower system implementation costs, which has been widely applied in many practical applications, like public safety and emergency response, autonomous driving and navigation [6], [7].

Recent efforts have revealed that the geometric configuration of the MR-RPS can significantly impact its capabilities to provide positioning service [8], [9], [10]. However, most existing studies on the optimal deployment problem focus on serving a single specific user within the mission space—commonly referred to as target localization—by employing various metrics [11], [12], [13], [14] and diverse optimization methodologies [15], [16], [17]. In contrast, the optimal deployment problem for the MR-RPS aims to determine an optimal geometric configuration that enhances the localization performance of stochastically appearing users, rather than focusing solely on a specific user. As a major compliment, [18] first presented the full concept of the optimal deployment problem of the range-measurement-based MR-RPS and proposed a novel deployment strategy by formulating the problem into an integrated locational optimization problem under the coverage control architecture. The key idea of this approach involves integrating the localization metric across the entire mission space, weighted by the user's probability of appearance, thereby substantially increasing the complexity of optimizing robot deployment.

This work attempts to extend the optimal deployment problem in [18] to bearing-based MR-RPS. Specifically, we apply the MRS equipped with bearing-only-measurement devices (e.g. cameras), for the propagation of location information from the MRS to the users, instead of distance-based measurements as studied in [18]. This setup can offer cost-effective and low-power advantages for the MRS configuration. Furthermore, as a passive optical sensor, the camera-based measurement system enables the simultaneous monitoring of both cooperative and non-cooperative users, thereby extending the applications of the MR-RPS. In this work, the localization performance is characterized by the integration of the FIM field given a known user's distribution. Through theoretical derivations, it is shown that a numerical gradient ascent-based pose update strategy can iteratively compute and adjust the optimal geometric configuration within the mission space, thereby providing optimal positioning services for all users.

The main contributions of this work are:

1) The optimal deployment problem for bearing-based MRS subject to both field-of-view and visibility constraints

Received 18 April 2025; accepted 2 August 2025. Date of publication 2 September 2025; date of current version 8 September 2025. This article was recommended for publication by Associate Editor G. Pereira and Editor M. Ani Hsieh upon evaluation of the reviewers' comments. This work was supported in part by the State Key Laboratory of Micro-Spacecraft Rapid Design and Intelligent Cluster under Grant MS01240110, in part by the National Natural Science Foundation of China under Grant 62303002, in part by the Key Program of Natural Science Foundation of Anhui Higher Education Institutions of China under Grant 2022AH050068. *(Corresponding author: Liang Zhang.)*

The authors are with the School of Electrical Engineering and Automation, Anhui University, Hefei 230093, China (e-mail: 1980464625@qq.com; liangzhang@ahu.edu.cn; wukeyue66@163.com; 1760756455@qq.com).

This article has supplementary downloadable material available at https://doi.org/10.1109/LRA.2025.3604740, provided by the authors.
Digital Object Identifier 10.1109/LRA.2025.3604740

TABLE I
COLLECTION OF NOTATIONS AND DEFINITIONS

Notation	Descriptions
$\boldsymbol{P}_i$	The joint pose vector for the i-th mobile robot
$\boldsymbol{P}$	The joint position and orientation vector for all $\boldsymbol{P}_i$
$\boldsymbol{P}_i^k$	The vector $\boldsymbol{P}_i$ at time step k
$\boldsymbol{V}$	A GNSS-limited mission space that is a 2-D $x-y$ plane
$\boldsymbol{V}_i$	The dominant region of the i-th mobile robot
$\mathcal{N}_i$	A subset of $\boldsymbol{V}_i$ overlaps with other robots
$\boldsymbol{T}$	A specific position in the mission space
$\phi(\boldsymbol{T})$	Density function to express the possibility of a user in $\boldsymbol{T}$
$\mathcal{C}$	The objection function of optimal deployment problem
$\mathcal{C}_i$	The objection function in $\boldsymbol{V}_i$
$\boldsymbol{\theta}$	The matrix of true relative angle between user and robots
$\boldsymbol{\omega}$	The noise from the bearing measurement
$\boldsymbol{e}_{1i}$	The unit vector from the i-th mobile robot to the user
$\boldsymbol{e}_{2i}$	The unit vector of the robot's heading direction

is modeled and formulated as a locational optimization problem utilizing the FIM metric, which extends the application of the MR-RPS.

2) A distributed deployment strategy is proposed, capable of iteratively and independently computing the position and orientation of all robots, thereby ultimately achieving the optimal geometric configuration for the MR-RPS.

II. Related Works

Optimal deployment for single target localization has been widely investigated during the last decades. In such scenarios, the target typically corresponds to the source (e.g., emitter). Therefore, multiple sensors (e.g, receiver) should be appropriately arranged to construct an optimal configuration for effective observation of the signal source, thereby reducing positioning errors. Existing research has predominantly focused on serving a single target; for example, [11], [12], [19], [20] investigate the optimal deployment of wireless sensors for better positioning precision of a single target node. It assumes that each sensor on the MRS can measure either the relative angle or distance to the target. Specifically, [12] examines the optimal sensor-target arrangements by measuring relative distances and employing the FIM and D-optimality criterion as metrics to evaluate the positioning accuracy. In addition, [11] adopts a hybrid measurement approach, obtaining both angle and distance information between sensors and targets. The optimal sensor placement strategy is derived by applying the Cramér-Rao lower bound (CRLB). More works investigate this problem by utilizing various positioning accuracy metrics, such as CRLB [21], Geometric Dilution of Precision (GDOP) [13], Position Dilution of Precision (PDOP) [14], and using diverse optimization methodologies, such as alternating direction method of multipliers [15], genetic algorithm [16], Particle Swarm Optimization [17].

This letter differs from the above studies in that the MR-RPS is responsible for handling targets appearing randomly anywhere in the mission space. As a result, the optimization must consider how the geometrical configuration affects positioning accuracy across all potential target locations, unlike the target localization case, which focuses only on accuracy at a single fixed point at the source.

III. Problem Formulation

Consider a set of N mobile robots equipped with bearing-measurement devices (e.g., cameras) in an GNSS-limited mission space moving on the 2-D $x-y$ plane $\boldsymbol{V} \subset \mathbb{R}^2$. These

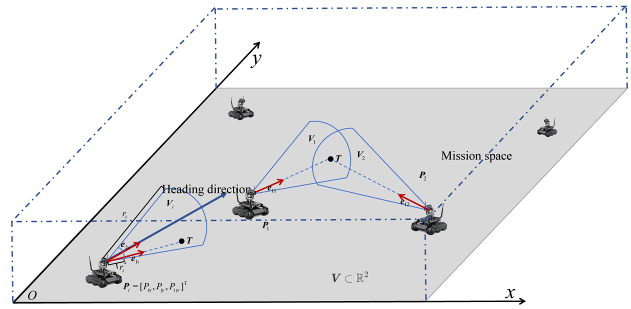

Fig. 1. 2-D space with notation definitions.

robots are deployed to provide positioning service for stochastically appearing users in the regional mission space by measuring the relative bearing, which is usually described by angle information between the mobile robot and the user. As depicted in Fig. 1, the pose of the i-th robot is denoted by $\boldsymbol{P}_i = [P_{ix}, P_{iy}, P_{i\psi}]^T$, $[P_{ix}, P_{iy}] \in \boldsymbol{V}$ represent the positions of the i-th robot and $P_{i\psi}$ is the heading angle. The joint position and orientation vector for all mobile robots in the mission space is formally defined as $\boldsymbol{P} = [\boldsymbol{P}_1, \boldsymbol{P}_2, \ldots, \boldsymbol{P}_N]^T \in \mathbb{R}^{3N \times 1}$.

In this letter, a density function $\phi(\boldsymbol{T})$ is applied to demonstrate the probability of the user appearing at the position $\boldsymbol{T} = [T_x, T_y]^T \in V$. In practice, the density function is positive and finite at all points in the mission space by its definition, i.e. $\phi(\boldsymbol{T}) > 0, \int_{\boldsymbol{V}} \phi(\boldsymbol{T}) d\boldsymbol{T} < \infty, \forall \boldsymbol{T} \in \boldsymbol{V}$. Without loss of generality, the Gaussian density function is applied:

$$\phi(\boldsymbol{T}) = k \cdot \exp\left(-\gamma \left\|\boldsymbol{T} - \boldsymbol{T}_d\right\|_2\right) \tag{1}$$

where k is a constant parameter, γ represents the parameter deciding the decay rate of the density distribution. Note that $\boldsymbol{T}_d$ here is the center with the highest probability that users may appear, rather than the position of a single user.

Inspired by [18], the optimal deployment problem of providing optimal positioning service for all stochastically appearing users in the mission space using the MR-RPS can be reformulated as the maximization of the following objective function by incorporating the coverage control theory.

$$\mathcal{C} = \int_{\boldsymbol{V}} \phi(\boldsymbol{T}) h(\boldsymbol{T}, \boldsymbol{P}) d\boldsymbol{T} \tag{2}$$

where $h(\boldsymbol{T}, \boldsymbol{P})$ is a metric for assessing the localization accuracy provided by a multi-sensor system for the user located at position $\boldsymbol{T}$.

Remark 1: Users assume dual roles: cooperative friendly units executing high-value tasks, or non-cooperative hostile entities. For cooperative roles, the MR-RPS functions as a mobile GPS, providing positioning/navigation signals. The relative user-robot positions can be mutually exchanged via communication. Conversely, when a robot detects a hostile entity, the MR-RPS should collaboratively maneuver to converge on the target for location and tracking. User appearance probabilities exhibit stochasticity in both scenarios. The probability density function $\phi(\cdot)$ provides prior knowledge of users' spatial distribution in the mission space. Lastly, the key distinction in optimal deployment between the MR-RPS and target localization [11], [12], [13], [14], [15], [16], [17], [19], [20], [21] lies in the integration of the localization performance weighted by user appearance probability in (2).

To evaluate the quality of the positioning service for a user $\boldsymbol{T} = [T_x, T_y]^T \in V$, we incorporate the FIM and D-optimality criteria, i.e., $\det(FIM)$. Therefore, the greater value of the indicator results in better positioning accuracy of the positioning service. Specifically, we first employ a generalized bearing model with an additive known Gaussian noise as inspired by [11]. Thereby, the bearing measurement between the i-th mobile robot and the user can be expressed as

$$\hat{\boldsymbol{\theta}} = \boldsymbol{\theta} + \boldsymbol{\omega} \tag{3}$$

where $\boldsymbol{\theta} = \left[\theta_1, \theta_2, \ldots, \theta_N\right]^T$ and $\theta_i = \tan^{-1}(\frac{T_y - P_{iy}}{T_x - P_{ix}})$ denotes the true relative angle between the user and the i-th mobile robot. $\boldsymbol{\omega} = \left[\omega_1, \omega_2, \ldots, \omega_N\right]^T$ stands for the noise from the bearing measurement. Without loss of generality, all ω_i are mutually independent and follow a Gaussian distribution with zero-mean and a variance of σ_i^2 i.e. $\omega_i \backsim \mathcal{N}(0, \sigma_i^2)$. Moreover, in this letter, we assume that all the bearing-measurement sensors equipped on the robots are the same i.e., $\sigma_1^2 = \sigma_2^2 = \cdots = \sigma_N^2 = \sigma^2$, which can be realized by applying identical bearing sensors on all robots. According to [11], the D-optimality $\det(FIM)$ is derived as

$$\begin{aligned} &\det(FIM) \\ &= \frac{1}{\sigma^4}\left(\sum_{i=1}^{N}\frac{\sin^2\theta_i}{d_i^2}\sum_{i=1}^{N}\frac{\cos^2\theta_i}{d_i^2} - \left(\sum_{i=1}^{N}\frac{\sin\theta_i\cos\theta_i}{d_i^2}\right)^2\right) \end{aligned} \tag{4}$$

where $d_i = \sqrt{(T_x - P_{ix})^2 + (T_y - P_{iy})^2}$ $i = 1, \ldots, N$ is the distance from user to i-th robot. Observed from (4), the quality of positioning service provided by the MR-RPS is mainly determined by the geometrical formation of MRS. As demonstrated in (4), the MR-RPS can continuously adjust their positions to derive a set of optimal observations for $\theta_i, d_i, \forall i \in [1, 2, \ldots, N]$, which results in an optimal observation geometry such that $\det(FIM)$ is maximized.

Remark 2: We opt to utilize the FIM to assess the accuracy of the positioning service. In comparison to PDOP and GDOP, FIM serves as a metric to assess the precision and effectiveness of parameter estimation. Specifically, the $\det(FIM)$ represents the amount of information contained in the observed data regarding the model parameters. A larger information quantity indicates that the parameters can be estimated with greater accuracy. It considers not only the deployment methods of MRS but also the impact of various sources of uncertainty (such as sensor noise) on localization accuracy. On the other hand, PDOP and GDOP only translate the impact of MRS layout methods on localization precision, and can be considered as a special case of FIM under uniform noise conditions.

In conclusion, the purpose of this letter is to design a distributed deployment strategy that enables the MR-RPS to compute its deployment pose iteratively. This approach aims to achieve an optimized geometrical formation of observation capable of providing positioning services, given a known density function for the user appearance probability. This problem is formally formulated into the locational optimization problem as follows:

$$\begin{aligned} \boldsymbol{P} &= \arg\max_{\boldsymbol{P}} \int_{\boldsymbol{V}} \phi(\boldsymbol{T}) \det(FIM(\boldsymbol{T}, \boldsymbol{P})) d\boldsymbol{T} \\ \text{s.t.} &\quad [p_{ix}, p_{iy}] \in \boldsymbol{V} \;\; i = 1, 2, \ldots, N \end{aligned} \tag{5}$$

IV. Iterative Computation of the Optimal Deployment

There are several difficulties in addressing the integral optimization problem in (5). Firstly, it computes the integration of the FIM across all locations within the mission space. Analyzing the impact of a single robot's positional change on the optimization objective is highly challenging, as the positions of all robots are required for the computation of the FIM. Secondly, the calculation of the FIM for a user position in the mission space requires at least two or more robots to observe the position point simultaneously. Otherwise, the FIM will fail to meet the rank requirement, leading to a singular solution in the computation. Finally, achieving the distributed optimization of the integral function (5) is still a non-trivial problem.

Regarding the problems mentioned above, this letter draws inspiration from the concept of *dominant region* in the coverage control problems in [18]. By transforming the observation boundary of most bearing-measuring equipment into the *dominant region* of the sensor for the segmentation of the mission space, we achieve the decoupling of the FIM from the motion of a single robot. Then, the original optimization problem is refined by mapping the singular cases in calculating the FIM to a monotonically increasing function. Consequently, the distributed deployment strategy is derived by a random-perturbation-based numerical gradient-ascending method.

A. Segmentation of the Mission Space

As is shown in Fig. 1, we model the limited field of vision (FOV) of the bearing-measurement devices into the *dominant region* of the i-th mobile robot, which is defined by the visual range of the i-th mobile robot as $\boldsymbol{V}_i \subset \boldsymbol{V}$. The regions in the mission space that are not observed by any mobile robot can be represented as $\boldsymbol{V}_0 := \{\boldsymbol{V}_0 | \boldsymbol{V}_0 \subset \boldsymbol{V}, \boldsymbol{V}_0 \cap \boldsymbol{V}_i = \varnothing, \forall i \in \{1, 2, \ldots, N\}\}$. Therefore, we have $\boldsymbol{V}_0 \cup \boldsymbol{V}_1 \cup \cdots \cup \boldsymbol{V}_N = \boldsymbol{V}$. To better describe the range of $\boldsymbol{V}_i$, we consider that all bearing-measurement devices are identical; we denote r as the maximum visibility range of the bearing-based devices. Additionally, we use α to represent the angle of the FOV of the bearing measurement sensors on the mobile robot. The bearing-measurement sensors could not measure the user who doesn't belong to their dominant region. Let denote $\boldsymbol{e}_{1i}$ the unit vector from the i-th mobile robot $\boldsymbol{P}_i$ to user $\boldsymbol{T}$, i.e.,

$$\boldsymbol{e}_{1i} = \boldsymbol{e}_{\boldsymbol{P}_i \to \boldsymbol{T}} = \frac{\boldsymbol{T} - \boldsymbol{P}_i}{\|\boldsymbol{T} - \boldsymbol{P}_i\|_2} \tag{6}$$

where $\|\boldsymbol{T} - \boldsymbol{P}_i\|_2$ represents the distance from $\boldsymbol{T}$ to $\boldsymbol{P}_i$ in mission space. Besides, we define the unit vector of the robot's heading direction as $\boldsymbol{e}_{2i} = [\cos \boldsymbol{P}_{i\psi}, \sin \boldsymbol{P}_{i\psi}]$. Then angle between the vector $\boldsymbol{e_{1i}}$ and the vector $\boldsymbol{e}_{2i}$ is

$$\theta \left\langle \boldsymbol{e}_{1i}, \boldsymbol{e}_{2i} \right\rangle = \cos^{-1}(\boldsymbol{e}_{1i} \cdot \boldsymbol{e}_{2i}) \tag{7}$$

Then we say that a user T is served or measured by robot i *if* $0 \le \theta \left\langle \boldsymbol{e}_{1i}, \boldsymbol{e}_{2i} \right\rangle \le \frac{\alpha}{2}$ and $r^* < \|\boldsymbol{T} - \boldsymbol{P}_i\|_2 \le r$, where r^* denotes the distance of measurement blind zone when the target is in close proximity to the sensor. Then we can formally defined the *dominant region* of i-th robot $\boldsymbol{V}_i = \{\forall \boldsymbol{T} \in \boldsymbol{V} | 0 \le \theta \left\langle \boldsymbol{e}_{1i}, \boldsymbol{e}_{2i} \right\rangle \le \frac{\alpha}{2} \cap r^* < ||\boldsymbol{T} - \boldsymbol{P}_i||_2 \le r\}$. In addition, we denote $\boldsymbol{N}_T^k = \{\forall \boldsymbol{P}_i \in \boldsymbol{P} | 0 \le \theta \left\langle \boldsymbol{e}_{1i}, \boldsymbol{e}_{2i} \right\rangle \le \frac{\alpha}{2} \cap r^* < ||\boldsymbol{T} - \boldsymbol{P}_i||_2 \le r\}$ as the set containing all mobile robots capable of observing the user $\boldsymbol{T}$ at time step k, whose size is N_T^k.

B. Transformation and Optimization of Coverage Function

To address the optimization problem in (5), it is necessary to precisely compute the FIM at each point in the mission space, given the robot locations $\boldsymbol{P}$. However, introducing the *dominant region* results in parts of the mission space being inadequately served, i.e., only one robot or no robot observes the area. Besides, the expansion of the D-optimality of the FIM in (4) exhibits abnormal behaviour when the distances between robots and the target approach zero.

To mitigate this issue, we propose a piecewise function $f(\cdot)$ to deal with the singularity cases with few robots and a continuously monotone-increasing function $g(\cdot)$ to map the quality of service $\det(FIM)$ into a smoother space, which can prevent the robot from approaching the target too closely. Considering the segmentation in the previous subsection, we can consequently reformulate the positioning service problem by maximizing the following alternative optimization problem:

$$\begin{cases} \mathcal{C} = \sum_{i=1}^{N} \mathcal{C}_i \\ \mathcal{C}_i = \int_{\boldsymbol{V}_i} \phi(\boldsymbol{T}) f(\det(FIM(\boldsymbol{T},\boldsymbol{P})))d\boldsymbol{T} \end{cases} \tag{8}$$

and

$$f(\cdot) = \begin{cases} 0, & \text{if } N_T^k = 0 \\ a, & \text{if} N_T^k = 1 \\ g(\det(FIM)), & \text{if } N_T^k \geq 2 \end{cases} \tag{9}$$

where a is a number that exhibits a positive correlation with $\phi(\boldsymbol{T})$ whose magnitude is significantly less than $\det(FIM)$ and $g(\det(FIM))$ is the monotonically increasing function inspired by the literature [18].

Remark 3: When using the FIM as the accuracy metric, it is crucial to recognize that users closer to mobile robots typically receive more accurate positioning information. According to our objective function, mobile robots tend to gravitate toward the centers of density center, potentially neglecting the likelihood of the user appearing near the center of density. To prevent positioning resources from being overly concentrated at the single point, we introduce the function $g(\det(FIM))$, which is an increasing function that maps the wide range of $g(\det(FIM))$ values into a much narrower interval, thereby preventing excessive or insufficient positioning information in certain areas. This approach enhances the overall reliability and fairness of the positioning service.

Remark 4: Accurate user positioning with mobile robots equipped with bearing measurement sensors requires at least two robots to obtain reliable relative bearing measurements, as a single robot cannot provide sufficient information for precise localization. To address this, a minimal value, significantly smaller than $g(\det(FIM))$, is assigned to $\mathcal{C}$ for users observed by a single robot. This ensures that robots autonomously move toward the center of the density function with higher positioning demands in the absence of overlapping observations.

C. Gradient Derivation Method

In the previous sections, we refined the objective function in (8) to address practical difficulties. This subsection presents a distributed deployment strategy for the optimization of the MR-RPS based on the numerical gradient ascent method. Specifically, the location iteration of i-th robot is updated by:

$$\boldsymbol{P}_i^{k+1} = \boldsymbol{P}_i^k + \left[\lambda_x \frac{\partial \mathcal{C}(\boldsymbol{P})}{\partial P_{ix}^k}, \lambda_y \frac{\partial \mathcal{C}(\boldsymbol{P})}{\partial P_{iy}^k}, \lambda_\psi \frac{\partial \mathcal{C}(\boldsymbol{P})}{\partial P_{i\psi}^k}\right] \tag{10}$$

where k is the time step, λ_x and λ_y are the rates of updating of mobile position, and λ_ψ is the rate of updating the orientation angle of mobile robots.

We employ the numerical gradient computation methods to efficiently compute each mobile robot's partial derivative, inspired by [22]. Let denote the perturbations $\boldsymbol{\Delta}_{ix} \in \mathbb{R}^{3N\times 1}$ as the vector containing all zero elements except for Δx_i of the x-axis element corresponding to i-th robot, i.e.,

$$\boldsymbol{\Delta}_{ix} = \Bigg[\underbrace{\mathbf{0}_{3\times 1}}_{1^{st} robot}, \underbrace{\mathbf{0}_{3\times 1}}_{2^{nd} robot}, \ldots, \underbrace{\Delta x_i, 0, 0,}_{i^{st} robot} \cdots\Bigg] \tag{11}$$

and denote

$$\boldsymbol{\Delta}_{iy} = \Bigg[\underbrace{\mathbf{0}_{3\times 1}}_{1^{st} robot}, \underbrace{\mathbf{0}_{3\times 1}}_{2^{nd} robot}, \ldots, \underbrace{0, \Delta y_i, 0,}_{i^{st} robot} \cdots\Bigg]$$

$$\boldsymbol{\Delta}_{i\psi} = \Bigg[\underbrace{\mathbf{0}_{3\times 1}}_{1^{st} robot}, \underbrace{\mathbf{0}_{3\times 1}}_{2^{nd} robot}, \ldots, \underbrace{0, 0, \Delta \psi_i,}_{i^{st} robot} \cdots\Bigg] \tag{12}$$

the vector for $\Delta y_i, \Delta z_i$ of the y and z axis, where $\Delta x_i, \Delta y_i, \Delta \psi_i$ are some small perturbations. Then, the numerical gradient is computed as follows:

$$\begin{aligned} \frac{\partial \mathcal{C}(\boldsymbol{P}^k)}{\partial P_{ix}^k} &= \frac{\mathcal{C}\left(\boldsymbol{P}^k + \boldsymbol{\Delta}_{ix}\right) - \mathcal{C}\left(\boldsymbol{P}^k\right)}{\Delta x_i} \\ \frac{\partial \mathcal{C}(\boldsymbol{P}^k)}{\partial P_{iy}^k} &= \frac{\mathcal{C}\left(\boldsymbol{P}^k + \boldsymbol{\Delta}_{iy}\right) - \mathcal{C}\left(\boldsymbol{P}^k\right)}{\Delta y_i} \\ \frac{\partial \mathcal{C}(\boldsymbol{P}^k)}{\partial P_{i\psi}^k} &= \frac{\mathcal{C}\left(\boldsymbol{P}^k + \boldsymbol{\Delta}_{i\psi}\right) - \mathcal{C}\left(\boldsymbol{P}^k\right)}{\Delta \psi_i} \end{aligned} \tag{13}$$

Remark 5: Note that the numerical gradient in (13) needs to acquire the deployment positions of all robots at the current moment to evaluate the overall objective in (8). This approach gathers the pose information from all robots into one central processor. However, in large-scale MR-RPS, this method can lead to network congestion and delays, negatively impacting real-time performance and responsiveness. Additionally, centralized control algorithms are heavily reliant on the central processor, making the system vulnerable to complete failure if the processor malfunctions. Therefore, it is important to develop a distributed strategy for optimal deployment.

Without loss of generality, we expand $\frac{\partial \mathcal{C}(\boldsymbol{P})}{\partial P_{ix}^k}$ by taking into consideration the definition of the objective function in (8) as follows:

$$\begin{aligned} \frac{\partial \mathcal{C}(\boldsymbol{P})}{\partial P_{ix}^k} &= \frac{\mathcal{C}(\boldsymbol{P}^k + \boldsymbol{\Delta}_{ix}) - \mathcal{C}(\boldsymbol{P}^k)}{\Delta x_i} \\ &= \frac{\mathcal{C}_i(\boldsymbol{P}^k + \boldsymbol{\Delta}_{ix}) - \mathcal{C}_i(\boldsymbol{P}^k)}{\Delta x_i} \end{aligned} \tag{14}$$

Therefore, by introducing the concept of the *dominant region*, we can decouple the calculation of the deployment strategy of the i-th robot from the uncovered area. To realize fully distributed computation of the numerical gradient, we emphasize that the computation of $\mathcal{C}_i$ can be reformulated into

$$\mathcal{C}_i = \int_{\boldsymbol{V}_i} \phi(\boldsymbol{T}) f(\det(FIM(\boldsymbol{T}, \boldsymbol{P}_i, \mathcal{N}_i)))d\boldsymbol{T} \tag{15}$$

where $\mathcal{N}_i = \{\boldsymbol{P}_j | \boldsymbol{V}_i \cap \boldsymbol{V}_j \neq \varnothing, \forall j \in \{1, \ldots, N\}, j \neq i\}$ is a subset of robots whose *dominant region* overlap with that of i-th robot. Note that this computation can be fully distributed if each robot equips a communication device with a maximum distance larger than $2r$. Then, the robots can share their poses with others within the communication range and select the neighboring set $\mathcal{N}_i$ according to its definition.

So far, we can design the control strategy for each robot as (10), with its gradient algorithm calculated by (13)–(15). This standard method employs the gradient ascent algorithm to maximize the objective function. However, the gradient magnitude varies with different initial conditions. Mobile robots positioned far from the density center typically experience a small gradient. In contrast, those near the density center encounter a significantly large gradient. Therefore, when a service regional mission space emerges, robots located at a far distance from the center of the density function will respond very slowly to the service demand. To address this challenge, we adopt a uniform step-size update approach. Let us denote $\Delta \boldsymbol{P}_i^k = \frac{\partial \mathcal{C}(\boldsymbol{P})}{\partial \boldsymbol{P}_i^k}$, then the gradient-based updated control strategy (10) is adapted to

$$P_{ix}^{k+1} = P_{ix}^k + \lambda_x \left(\frac{\Delta P_{ix}^k}{\left\| \Delta P_{ix}^k \right\|_2} + rs \right)$$
$$P_{iy}^{k+1} = P_{iy}^k + \lambda_y \left(\frac{\Delta P_{iy}^k}{\left\| \Delta P_{iy}^k \right\|_2} + rs \right)$$
$$P_{i\psi}^{k+1} = P_{i\psi}^k + \lambda_\psi \left(\frac{\Delta P_{i\psi}^k}{\left\| \Delta P_{i\psi}^k \right\|_2} + rs \right) \tag{16}$$

where the term rs is a small random number inspired by [22], which represents the product of a piecewise constant function and a value satisfying Brownian motion to avoid the local maximum traps. The final algorithm for the optimal deployment strategy is concluded in the Algorithm 1.

Remark 6: The gradient directions computed for the pose of each mobile robot based on (2) and (15) are theoretically identical. Here, (2) represents a globally defined coverage function, while (15) corresponds to a coverage function formulated for the i-th mobile robot and its neighboring agents, with the latter being a localized instantiation of the former. In practical implementations, provided that communication latency and information loss are eliminated, the gradient directions derived from theoretical calculations under both frameworks exhibit complete consistency. This alignment stems from the hierarchical relationship between the two formulations, where the local gradient computation in (15) inherently preserves the global optimality conditions embedded in (2) under ideal communication constraints.

Algorithm 1: Deployment Strategy of i-th Robot at Time k.

Require: λ_x, λ_y, λ_ψ, $\boldsymbol{P}_i^k$
Ensure: $\boldsymbol{P}_i^{k+1}$
1: Share its pose $\boldsymbol{P}_i^k$ via its communication device.
2: Receive the poses of other robots $\boldsymbol{P}_j^k$ within its communication range.
3: Compute $\boldsymbol{V}_i$ and $\boldsymbol{V}_j, \forall \boldsymbol{P}_j \in \mathcal{N}_j$ according to the segmentation model in Section III.A, and then calculate the neighboring set $\mathcal{N}_i$ according to its definition.
4: Compute the cost $\mathcal{C}_i$ by (15). The integration can be approximated by a numerical method, i.e., scatter the mission space into meshes, choose the central point $\boldsymbol{T}_m$ as the coordinate of the m-th mesh, calculate the $\det(FIM)$ by (4) for $\boldsymbol{T}_m$, and then sum up the multiplying value of the mesh size and $\phi(\boldsymbol{T}_m) f(\det(FIM(\boldsymbol{T}_m, \boldsymbol{P}_i, \mathcal{N}_i)))$ over all meshes $\forall \boldsymbol{T}_m \in \boldsymbol{V}_i$.
5: Compute the gradient by (13) and (14)
6: Compute the deployment strategy $\boldsymbol{P}_i^{k+1}$ by (16)
7: **Return:** $\boldsymbol{P}_i^{k+1}$

V. Simulation and Physical Experiment

We conducted two simulations and a physical experiment to validate the efficiency of the proposed deployment strategy. Firstly, the basic simulation with four robots serving a density function is used to show the correctness of the proposed deployment method. Then, the resilience of MR-RPS is assessed when any existing robot malfunctions or when the new robot is introduced. Lastly, we further validated the correctness and efficiency of our designed deployment strategy through physical experiments using multiple Turtlebots carrying cameras.

In the simulations, we consider a mission space $\boldsymbol{V} := \{[x, y] | 0 \leq x, y \leq 200\}$. The bearing measurement sensor used in this section is a camera whose maximum viewing radius r is 50, $r*$ is 0.1, and the horizontal field of view angle is $\frac{\pi}{3}$. Besides, we design the function $g(\cdot)$ is

$$g(x) = \mu - \frac{1}{e^{\gamma x}} \tag{17}$$

There are two parameters of the $g(\cdot)$. The parameter μ is utilized to holistically regulate the coverage function, and it is customary to adjust its value to ensure the function remains positive. The purpose of setting the value of γ is to modulate the rate of change of the $g(\cdot)$. This adjustment better reflects the influence of the mobile robot's pose on the objective function (8). In the following simulations and experiment, we set the parameters as $\mu = 2, \gamma = 10^5$ to prevent excessive growth acceleration as the green line in Fig. 2(c).

The center of the Gaussian density in (1) is [100,100]. Besides, the decay rate and the constant parameter are chosen as $k = 10$ and $\alpha = 1$. Adjustments can be made to the density center and α to delineate distinct users. The mesh size in Algorithm 1 influences both the accuracy and complexity of numerical integration calculations. Theoretically, a smaller mesh size enhances numerical precision and integration accuracy but necessitates increased computational time. To balance accuracy and efficiency, we discretize the mission space into 100×100 meshes. The values of λ_x, λ_y, and λ_ψ will influence the angular velocity and linear velocity of the robots. We set $\lambda_x = \lambda_y = 0.2$ and $\lambda_\psi = 0.04$ as the simulation parameter. The correctness and effectiveness are validated by presenting the change of the global coverage function (2). A larger value of this function indicates a better localization service.

A. Basic Simulation With Four Robots

In this simulation, we utilized four mobile robots with randomly initialized positions to perform the localization service for

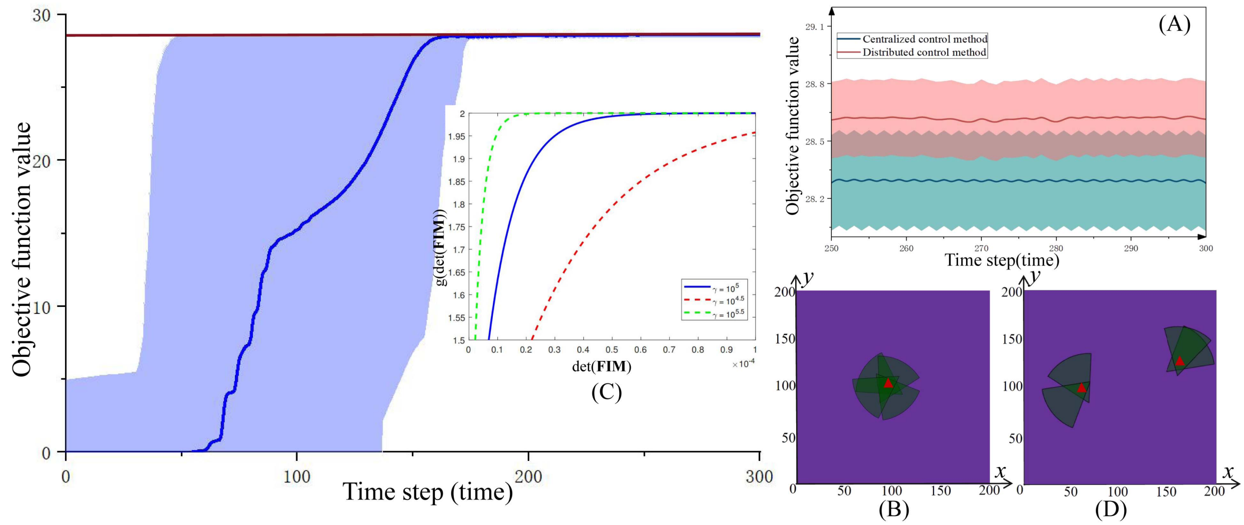

Fig. 2. Verification of the reliability of the control algorithm, (a) comparison between the centralized algorithm and the distributed algorithm, (b) is the final deployment strategy achieved by most trials, (c) is the parameters in $g(\det(FIM))$, (d) is the deployment strategy in the mission space have double density center.

the mission space. During the simulation, all four robots calculate their deployment strategies by Algorithm 1. The simulation was repeated 200 times. Each trial lasted for 300 time steps. The statistical results of the simulation are shown in Fig. 2. Furthermore, we derive the global optimal solution of the positioning problem by exhaustive searching using a genetic evolutionary algorithm. The value of the objective function corresponding to the global solution is shown by the solid red line in Fig. 2. We also use a centralized solution to operate the same simulation; the comparative result is presented in Fig. 2(a), which shows that the deployment strategy based on the distributed algorithm is better, which is attributed to the computational delays and decision errors. It requires global system modeling and centralized resources, leading to delays in large-scale deployments. Moreover, simultaneous decision-making in centralized algorithms often overlooks subsystem interactions, hindering global optimality. In contrast, distributed methods decentralize computations, allowing subsystems to independently select optimal strategies, resulting in better stability and feasibility.

We can observe from the results that the locational optimization objective function in (2) consistently increases and eventually converges across all 200 trials, despite different initial robots' poses. The final deployment strategy achieved by most trials is depicted in Fig. 2(b), where all four robots uniformly surround the center of density. Recalling the fact that our gradient-based deployment strategy is updated according to the modified coverage function in (15), the original objective for the MR-RPS positioning service in (2) can still be driven to a near-optimal solution, which validates the correctness and effectiveness of the proposed methods. Lastly, we operate the same simulation in the mission where have double density center [60,100] and [160,120], one optimal deployment strategy is shown in Fig. 2(d), the result is similar as the result in single density center that is more localization attention is allocated to areas near the density center. However, we note that the localization performance depend on the initial pose of the MRS. If all robots are initially deployed near one density center, users near others may lack positioning service. As density centers increase, more robots are required. Therefore, future work should prioritize initial distribution to ensure optimal coverage for all stochastic users.

B. Resilience to Robot Failure and Changing MRS Size

The purpose of this simulation is to validate the resilience of the MR-RPS that we designed. Initially, two mobile robots are randomly deployed in the mission space and autonomously adjust their placement within 300 steps by Algorithm 1 to provide the optimal positioning service. Subsequently, two additional robots are introduced, and the system reaches a new equilibrium within another 300 steps. Finally, we randomly remove a robot to simulate the case of node failure in a real scenario. This process is repeated for 50 trials with varying initial poses, and the results are shown in Fig. 3.

The initial 300 steps replicate the results of the first experiment, where two robots provide the optimal positioning service for random users by the deployment strategy in Algorithm 1, with their poses stabilizing as shown in Fig. 3(a). The addition of two more robots improved the MR-RPS overall performance, as illustrated in Fig. 3(b). When one robot fails, as depicted in Fig. 3(c), the positioning service performance declines, but the system remains functional, which demonstrates that the designed deployment strategy provides the MR-RPS with strong resilience.

C. Physical Verification Experiment

To further validate the feasibility of the proposed deployment strategy, we conducted a physical experiment.[1] The mission space is a 4 m × 4 m 2D plane in the room. We set the central point of the density function at the midpoint of the mission space. As done in the first simulation, we employed four mobile robots to provide positioning services using mounted cameras. The purpose for all four robots is to autonomously form an optimal observation geometry to optimize the locational

[1]More details about the physical experiment can be found in the attached multimedia materials, provided by the authors, including one video clip corresponding to the physical experiment.

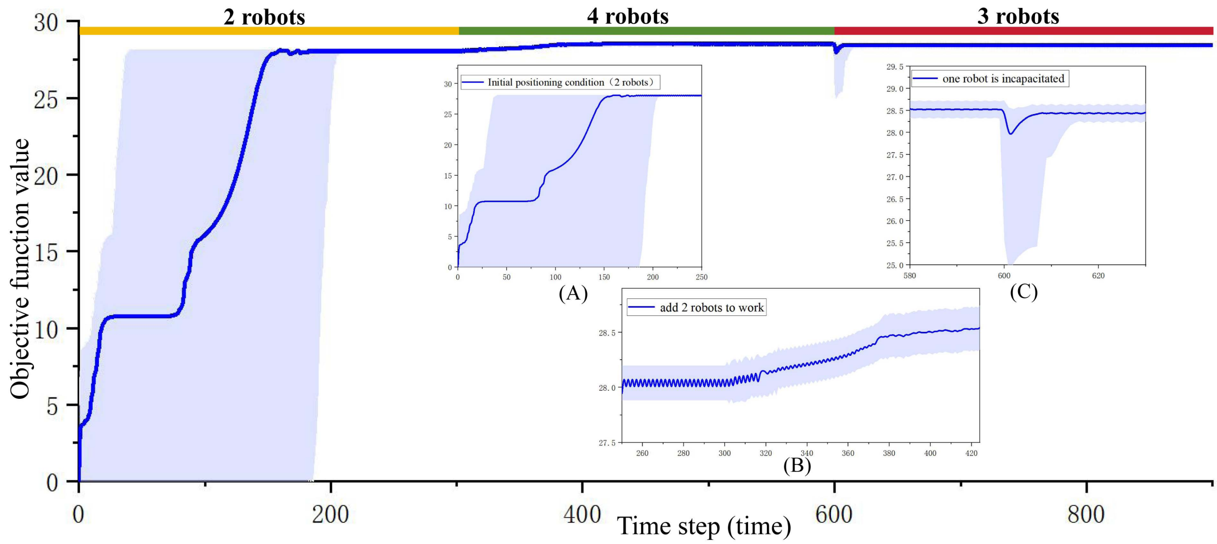

Fig. 3. Performance distribution map of the system positioning service when the mobile robot fails and joins, (a), (b) and (c) reveal the details at different times respectively.

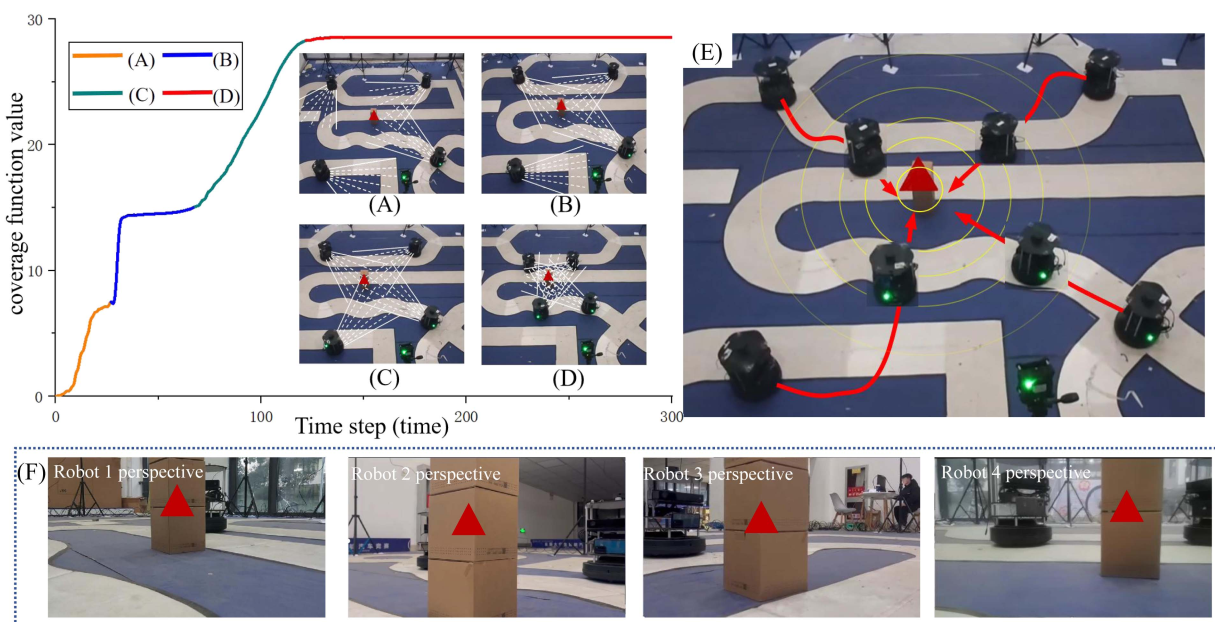

Fig. 4. Experimental results, (a)–(d) show the state of MRS at different moments, (e) is the moving trajectory of mobile robots, and (f) is the perspective of 4 mobile robots at the final moment.

objective function in (2). To obtain precise pose information for all mobile robots within the mission space, we employed the NOKOV optical motion capture system. This system uses precisely placed cameras to track reflective markers on the robots and calculate their poses with high accuracy.

In this experiment, the initial poses of the four robots are randomly generated at the four corners, as shown in Fig. 4. We utilized a workstation computer as the host and four mobile robots as clients. By establishing communication between the host and the clients, the workstation was able to control the mobile robots. The pose information of the mobile robots was collected by NOKOV and transmitted to the host. Based on the proposed deployment strategy, the host sent movement instructions to the clients. The robots ceased movement when their poses reached the state shown in Fig. 4, indicating that the optimal positioning service was achieved under these conditions. As shown in Fig. 4, the movement of the robots can be divided into four stages. In Fig. 4(a), the mobile robots start serving. The quality of localization service improves rapidly. This is attributed to the overlap of observation areas by neighboring robots, which converge towards the center of density function. In this time step, the MRS started offering positioning services if the user can be observed by at least two robots. Subsequently, the localization service performance experiences a significant leap, as shown in Fig. 4(b), due to three mobile robots providing positioning services to the user at the same time step. After reaching a stable state, in Fig. 4 (C), the fourth mobile robot joins the localization service, and all robots orient themselves towards the density function center while converging on it, thereby offering enhanced localization services. The final fields of view of the four mobile robots are presented in Fig. 4(f), and the movement trajectories of the four mobile robots are shown in Fig. 4(e); the red triangle is the density function center of the mission space. The entire physical experiment fully demonstrates that the proposed control algorithm enables the MR-RPS to achieve optimal positioning service.

VI. Conclusuion

In this letter, we propose a distributed deployment strategy to achieve optimal geometric configurations for the bearing-based MR-RPS, which can offer cost-effectiveness and energy efficiency through mounting low-cost bearing measurement sensors, such as cameras. The deployment strategy is validated by extensive results from simulation and physical experiment. The method proposed in this letter expands the application scenarios of the MR-RPS, enabling the system to be a more promising and economically viable alternative to the GNSS in critical scenarios.

Despite its advantages, the proposed control method has limitations. First, while perturbations are introduced during numerical gradient calculations, robots may still encounter local optima. Although data suggest near-global optimality, future work may explore the potential of achieving the globally optimal solution. Furthermore, the method assumes ideal pose information, overlooking localization uncertainties that could impact service quality. Besides, future research should focus on deriving analytical gradients of the FIM field using relative bearing measurements. Lastly, the optimization of other parameters, except extrinsics of robots, can be optimized within the field of MR-RPS.

References

[1] P.-W. Son, J. H. Rhee, and J. Seo, "Novel multichain-based Loran positioning algorithm for resilient navigation," *IEEE Trans. Aerosp. Electron. Syst.*, vol. 54, no. 2, pp. 666–679, Apr. 2018.

[2] X. Guo, K. Liu, Z. Meng, X. Li, and J. Yang, "Pseudolite-based lane-level vehicle positioning in highway tunnel," *IEEE Trans. Intell. Transp. Syst.*, vol. 25, no. 2, pp. 1612–1624, Feb. 2024.

[3] L. Zhao et al., "Vehicular computation offloading for industrial mobile edge computing," *IEEE Trans. Ind. Informat.*, vol. 17, no. 11, pp. 7871–7881, Nov. 2021.

[4] N. Mailhot and P. Gurfil, "Constellation design for regional space-Borne geolocation," *J. Guid., Control, Dyn.*, vol. 45, no. 5, pp. 795–814, 2022.

[5] L. N. Lysenko, V. V. Koryanov, and A. G. Toporkov, "The analysis of possibility of integration the global information satellite systems second generation with regional systems on the basis of modern small and micro spacecrafts," in *Proc. IEEE Int. Conf. Mech., Syst. Control Eng.*, 2017, pp. 310–318.

[6] G. Zhang, W. Wen, B. Xu, and L.-T. Hsu, "Extending shadow matching to tightly-coupled GNSS/INS integration system," *IEEE Trans. Veh. Technol.*, vol. 69, no. 5, pp. 4979–4991, May 2020.

[7] D. Lee, H. Seong, G. Kang, S. Han, D. H. Shim, and Y. Yoon, "Design, field evaluation, and traffic analysis of a competitive autonomous driving model in a congested environment," *IEEE Trans. Intell. Transp. Syst.*, vol. 25, no. 8, pp. 9482–9497, Aug. 2024.

[8] Y. Wang, K. Gu, Y. Wu, W. Dai, and Y. Shen, "NLOS effect mitigation via spatial geometry exploitation in cooperative localization," *IEEE Trans. Wireless Commun.*, vol. 19, no. 9, pp. 6037–6049, Sep. 2020.

[9] S. Tomic and M. Beko, "A geometric approach for distributed multi-hop target localization in cooperative networks," *IEEE Trans. Veh. Technol.*, vol. 69, no. 1, pp. 914–919, Jan. 202.

[10] W. Li, M. Liu, T. Chen, and G. Mao, "Vehicles selection algorithm for cooperative localization based on stochastic geometry in Internet of vehicle systems," *IEEE Trans. Veh. Technol.*, vol. 74, no. 3, pp. 4893–4903, Mar. 2025.

[11] S. Xu, "Optimal sensor placement for target localization using hybrid RSS, AOA and TOA measurements," *IEEE Commun. Lett.*, vol. 24, no. 9, pp. 1966–1970, Sep. 2020.

[12] M. Sadeghi, F. Behnia, and R. Amiri, "Optimal geometry analysis for TDOA-based localization under communication constraints," *IEEE Trans. Aerosp. Electron. Syst.*, vol. 57, no. 5, pp. 3096–3106, Oct. 2021.

[13] S.-H. Bach and S.-Y. Yi, "Constrained least-squares trilateration for indoor positioning system under high GDOP condition," *IEEE Trans. Ind. Informat.*, vol. 20, no. 3, pp. 4550–4558, Mar. 2024.

[14] Y. Li, Z. Zhang, X. He, Y. Wen, and X. Cao, "Realistic stochastic modeling considering the PDOP and its application in real-time GNSS point positioning under challenging environments," *Measurement*, vol. 197, 2022, Art. no. 111342.

[15] N. Sahu, L. Wu, P. Babu, B. S. MR, and B. Ottersten, "Optimal sensor placement for source localization: A unified ADMM approach," *IEEE Trans. Veh. Technol.*, vol. 71, no. 4, pp. 4359–4372, Apr. 2022.

[16] S. Haigh, J. Kulon, A. Partlow, and C. Gibson, "Comparison of objectives in multiobjective optimization of ultrasonic positioning anchor placement," *IEEE Trans. Instrum. Meas.*, vol. 71, 2022, Art. no. 2513212.

[17] W.-N. He, X.-L. Huang, Z. Xu, F. Hu, and S. Yu, "Adaptive anchor deployment for diverse demands on localization precision," *IEEE Trans. Veh. Technol.*, vol. 73, no. 12, pp. 19480–19494, Dec. 2024.

[18] L. Zhang, Z. Zhang, R. Siegwart, and J. J. Chung, "Distributed PDOP coverage control: Providing large-scale positioning service using a multi-robot system," *IEEE Robot. Automat. Lett.*, vol. 6, no. 2, pp. 2217–2224, Apr. 2021.

[19] J. J. Khalife and Z. Z. M. Kassas, "Optimal sensor placement for dilution of precision minimization via quadratically constrained fractional programming," *IEEE Trans. Aerosp. Electron. Syst.*, vol. 55, no. 4, pp. 2086–2096, Aug. 2019.

[20] M. Sadeghi, F. Behnia, and R. Amiri, "Optimal sensor placement for 2-D range-only target localization in constrained sensor geometry," *IEEE Trans. Signal Process.*, vol. 68, pp. 2316–2327, 2020.

[21] S. Xu, L. Wu, K. Doğançay, and M. Alaee-Kerahroodi, "A hybrid approach to optimal TOA-sensor placement with fixed shared sensors for simultaneous multi-target localization," *IEEE Trans. Signal Process.*, vol. 70, pp. 1197–1212, 2022.

[22] S. H. Kang, S. J. Kim, and H. Zhou, "Optimal sensor positioning; a probability perspective study," *SIAM J. Sci. Comput.*, vol. 39, no. 5, pp. B759–B777, 2017.